(in preparation for *Chemosphere* Special Issue on Atmospheric Carbon Monoxide)

Measurements of CO in the Upper Troposphere and Lower Stratosphere

R. L. Herman[1], C. R. Webster[2], R. D. May[2], D. C. Scott[2], H. Hu[2], E. J. Moyer[1], Y. L. Yung[1], P. O. Wennberg[1], T. F. Hanisco[3], E. J. Lanzendorf[3], R. J. Salawitch[2], J. J. Margitan[2], and T. P. Bui[4]

[1]Division of Geological and Planetary Sciences, California Institute of Technology, Pasadena, CA 91125.

[2]Jet Propulsion Laboratory, California Institute of Technology, Pasadena, CA 91109.

[3]Atmospheric Research Project, Harvard University, Cambridge, MA 02138.

[4]NASA Ames Research Center, Moffett Field, CA 94035.

Abstract. *In situ* measurements of CO were made in the upper troposphere and lower stratosphere (7 to 22 km altitude) with the JPL Aircraft Laser Infrared Absorption Spectrometer (ALIAS) on 58 flights of the NASA ER-2 aircraft from October 1995 through September 1997, between 90°N and 3°S latitude. Measured upper tropospheric CO was variable and typically ranged between 55 and 120 ppb, except for higher values over Alaska during summer 1997. Tropical stratospheric CO ranged from 58±5 ppb at the tropopause to 12±2 ppb above 20 km, having similar profiles in all seasons of the year. The tropical profile is reproduced by a simple model of tropical ascent using measured OH, model Cl and O(^{1}D), and diabatic heating rates from a radiative heating model. At the highest ER-2 altitudes, measured CO was close to the calculated steady-state mixing ratios of 10 to 15 ppb; however, in the lowermost stratosphere, CO was far from

photochemical equilibrium. Calculations of photochemical loss of CO indicate that quasi-horizontal transport from the tropics to the mid-latitude lower stratosphere occurs on a time scale of one month or less for the region of the stratosphere between 380 K and 450 K potential temperature.

Introduction

Carbon monoxide (CO) plays a central role in atmospheric photochemistry. It has long been recognized that CO is the dominant sink of tropospheric OH, the primary oxidant in the troposphere [*Levy*, 1971]. CO also contributes to O_3 production in the troposphere [*Crutzen*, 1995; *Wennberg et al.*, 1998], and potentially in the lowermost stratosphere as well [*Bregman et al.*, 1997]. In the troposphere, the dominant sources of CO are oxidation of CH_4 and other hydrocarbons, biomass burning, and direct anthropogenic emissions [*Logan et al.*, 1981]. In the lower stratosphere, the dominant sources of CO are transport from the CO-rich boundary layer [*Harriss et al.*, 1992] and local production from CH_4 [*Pinto et al.*, 1983; *Logan et al.*, 1981]. CH_4 is oxidized in a series of fast photochemical reactions initiated by:

$$CH_4 + X \rightarrow CH_3 + HX \qquad \text{where X = OH, O(}^1\text{D), or Cl} \qquad (1)$$

where CH_4 + OH is the dominant reaction. Reaction (1) is the rate-limiting step in CO production from CH_4, and has a strong temperature-dependence for X = OH or Cl. Subsequent steps rapidly produce CH_2O, which is then photolyzed to CO, the longest-lived intermediate in the oxidation pathway from CH_4 to CO_2.

The CO photochemical lifetime is determined by reaction with OH [*Logan et al.*, 1981; *Pressman and Warneck*, 1970]:

$$CO + OH \rightarrow CO_2 + H \qquad (2)$$

In the lower stratosphere, the CO mixing ratio is much greater than its steady-state value due to transport across the tropopause. As air ascends in the tropics, there is CO loss by reaction (2) and a small source from reaction (1). The net rate of change of CO is thus:

$$\frac{d[CO]}{dt} = -k_2[CO][OH] + [CH_4]\{k_{OH}[OH] + k_{Cl}[Cl] + k_{O1D}[O^1D]\} \qquad (3)$$

In the absence of mixing, stratospheric CO decreases exponentially until photochemical steady-state is reached. Hence, in the stratosphere, elevated CO can be used as a tracer of air that recently came from the troposphere.

Aircraft *in situ* measurements of atmospheric CO have the potential to improve our understanding of stratosphere-troposphere exchange and transport within the lower stratosphere because CO has a sharp gradient across the tropopause and a photochemical lifetime of only a few months. Aircraft have excellent vertical resolution of the near-tropopause region compared to satellites, and wide enough spatial coverage to carry out studies on regional to hemispheric scales. There have been many aircraft studies of CO up to 12.5 km [e.g. *Hoor et al.*, this issue; *Waibel et al.*, this issue; *Lelieveld et al.*, 1997; *Anderson et al.*, 1993], but the NASA ER-2 aircraft has made possible *in situ* measurements up to 22 km altitude. The ER-2 database is unique in the large number of trace gases that are measured simultaneously with particle concentration, solar irradiance, and meteorological variables [*Tuck et al.*, 1997]. Aboard the ER-2, the Aircraft Laser

Infrared Absorption Spectrometer (ALIAS) of the Jet Propulsion Laboratory (JPL) simultaneously measures CO, N_2O, CH_4, and NO_2 or HCl [*Webster et al.*, 1994] with high precision and accuracy (see below) and fast response (3 sec). In 1995-7, ALIAS collected data on 58 ER-2 flights during two NASA campaigns: Stratospheric TRacers of Atmospheric Transport (STRAT) in 1995-6 and Photochemistry of Ozone Loss in the Arctic Region In Summer (POLARIS) in 1997. This paper describes the spatial distribution of upper tropospheric and lower stratospheric CO measured by ALIAS. In addition, a simple model is used to constrain the CO photochemical lifetime and estimate horizontal transport time scales in the lower stratosphere.

Aircraft Instruments

ALIAS is a high-resolution, scanning, mid-infrared absorption spectrometer that has four tunable diode lasers (TDLs) to simultaneously measure CO, N_2O, CH_4, and NO_2 or HCl [*Webster et al.*, 1994; *May and Webster*, 1993]. The instrument uses harmonic spectroscopy to achieve high sensitivity: absorptions as small as 1 part in 10^5 can be detected in a 3-sec integration period. The signal is amplified, filtered, and demodulated at twice the laser modulation frequency to yield second-harmonic spectra. Each of the four channels has an InSb or HgCdTe detector mounted inside the same liquid nitrogen dewar as the TDLs. Thirty spectral scans are averaged together and written to a hard disk every 3 sec along with laser power, detector zero level, pressure, gas temperature, component temperatures, and heater powers.

The instrument is mounted in a pod on the right wing of the ER-2. Air is sampled isokinetically through a heated inlet probe in front of the wing pod and flows through a 1-m absorption cell with a flush time of 1 to 2 sec. An instrument response time of 3 sec. allows high spatial resolution along the ER-2 flight path. Within the absorption cell, the infrared laser beams are reflected 80 times between two Au-coated spherical aluminum mirrors in a Herriott cell multipass optical configuration to achieve an 80-m optical pathlength. For CO, the instrument precision (±1 st. dev.) is ±0.7 parts per billion by volume (ppb) for 3-sec average data. For ground calibration, we use gas standards provided by the National Oceanic and Atmospheric Administration (NOAA) Climate Monitoring and Diagnostics Laboratory (CMDL). The gas standards are introduced into the absorption cell and spectra are taken over the range of pressures expected during flight. The estimated instrument accuracy is ±5% relative to these calibration standards.

For the following analysis, we use simultaneous ER-2 measurements of CO, CH_4, OH, H_2O, O_3, temperature, pressure, and tropopause height. The Harvard HO_x instrument uses laser-induced fluorescence to detect OH radicals [*Wennberg et al.*, 1994]. H_2O is measured by the Harvard H_2O instrument with Lyman-α photofragment fluorescence [*Weinstock et al.*, 1994] and also by the JPL H_2O instrument using near-infrared TDL spectroscopy [*May*, 1998]. The JPL O_3 instrument measures O_3 by ultraviolet absorption spectroscopy [*Proffitt and McLaughlin*, 1983]. Temperature and pressure are measured by the ER-2 Meteorological Measurement System (MMS) [*Scott et al.*, 1990]. The Microwave Temperature Profiler (MTP) is a passive microwave radiometer that measures O_2 thermal emission to calculate temperature profiles, thereby determining the local tropopause height [*Denning et al.*, 1989].

CO Distribution

ALIAS has measured CO in the upper troposphere (above 7 km) and lower stratosphere (up to 22 km) during the STRAT and POLARIS campaigns. In the upper troposphere, CO varies considerably on daily to seasonal time scales [*Logan et al.*, 1981, and references therein]. Figure 1 shows monthly distributions of upper tropospheric CO measured at three latitudes: 65°N near Fairbanks, AK, 37°N near NASA Ames, CA, and 21°N near Barber's Point, HI. The data included in this figure were taken between 7 km altitude and the local tropopause minus 1 km. Tropopause heights were determined from temperature profiles measured by the MTP and MMS instruments aboard the ER-2 [*B. L. Gary*, pers. comm.]. There is generally less CO in the upper troposphere than in the marine boundary layer because most CO production is in the boundary layer [*Logan et al.*, 1981]. As shown in Figure 1, upper tropospheric CO generally increases with latitude in the Northern Hemisphere [*Robinson et al.*, 1984, and references therein]. Since the instrument precision is ±0.7 ppb CO, scatter within each month of data is caused by atmospheric variability. The striking summer maximum of CO over Alaska is likely due to forest fires, which efficiently loft material to the upper troposphere [*Waibel et al.*, this issue]. The Alaska measurements taken in June and July, 1997, are similar to 1995 ground-based observations from Fairbanks [*L. Yurganov*, pers. comm.]. Such high mixing ratios of CO may lead to significant O_3 production in the upper troposphere [*Fishman and Crutzen*, 1978]. In April and September, there is considerably less CO in the high latitude upper troposphere.

In California (37°N), upper tropospheric CO has an annual maximum of 85 to 100 ppb in late autumn and winter, and a minimum of 60 to 70 ppb in spring (Figure 1). In Hawaii (21°N), upper tropospheric CO is typically 60 to 80 ppb with a similar seasonal cycle. At both locations, synoptic-scale dynamics and stratosphere-troposphere exchange cause variability in CO. Stratosphere-troposphere exchange can be identified by the measured O_3 *vs.* CO relationship because these species are strongly anticorrelated in the lower stratosphere (Figure 2a) [e.g. *Hipskind et al.*, 1987]. The O_3 mixing ratio at the tropopause is typically 100 to 150 ppb in these data measured over Hawaii in November, 1995, and December, 1996. More than 1 km below the local tropopause, O_3 and CO are not strongly correlated in the upper troposphere except during the flights of 961208 and 961209 (yymmdd format). Pollution and biomass burning are associated with elevated O_3 and CO, while the background troposphere has relatively little O_3 and CO, so high O_3 (> 150 ppb) and low CO (< 40 ppb) uniquely identify stratospheric air in the upper troposphere.

Tropical CO was measured by ALIAS on five ER-2 flights from Hawaii to the equator (see Figure 3). Close to the equator, the aircraft descends from its cruise altitude of 21 km to a minimum altitude of 15 km, and then climbs back to 21 km. In this way, vertical profiles are obtained of the tropical lower stratosphere and upper troposphere. We found that CO is less variable in the tropics than at higher latitudes in the Northern Hemisphere. Over the central tropical Pacific Ocean (10°N to 3°S, 150 to 160°W), measured upper tropospheric CO is 60±5 ppb with no apparent seasonal variation. These mixing ratios are representative of the background tropical troposphere away from biomass burning plumes [*P. Novelli*, pers. comm.].

In the tropical lower stratosphere, the CO mixing ratio decays with altitude due to photochemical loss. The vertical profile of CO is strongly affected by seasonal variations in tropopause height (Figure 3a). However, the potential temperature of the tropical tropopause varies less than tropopause height does [*Reid and Gage*, 1996] (potential temperature is defined as the temperature of an air parcel adiabatically compressed or expanded to 1000 hPa). Potential temperature, θ, is a Lagrangian tracer of adiabatic motion and is conserved on time scales of approximately two weeks. The CO profile in the tropics varies little with season if θ is the vertical coordinate (Figure 3b). CO and θ are strongly anticorrelated in the tropics because diabatic heating increases θ while photochemistry decreases the CO mixing ratio. The mean tropical tropopause of these ER-2 flights is at $\theta \approx 370 \pm 10$ K (altitudes ranging from 15.5 to 17.2 km) with a corresponding CO mixing ratio of 58±5 ppb. By θ = 390 K, tropical air has only 45±5 ppb CO. The lowest mixing ratios measured by ALIAS in the tropics are 12±2 ppb at altitudes above 20 km (θ > 470 K). *Weinstock et al.* [1998] used the functional relationship between CO and θ as a photochemical clock to infer the stratospheric age of air parcels. We will demonstrate below that tropical CO loss is consistent with measured OH and calculated heating rates.

From the perspective of transport, the stratosphere can be divided into two layers based on potential temperature. The "overworld" is defined by θ > 380 K, and the stratospheric "middleword" is bounded above by the θ = 380 K isentrope (i.e. surface of constant θ) and below by the extra-tropical tropopause [*Holton et al.*, 1995; *Hoskins*, 1991]. In the extra-tropics, stratosphere-troposphere exchange is thought to occur by

adiabatic quasi-horizontal mixing along isentropes, tropopause folding, and convection [*Holton et al.*, 1995, and references therein]. However, none of these mechanisms can transport significant material above the middleworld. Only in the tropics is there strong enough diabatic heating for air parcels to ascend into the overworld. It is a seeming contradiction that up to 50% of the air in the tropical overworld has been entrained from the extra-tropical stratosphere [e.g. *Volk et al.*, 1996]. However, this entrainment is nearly isentropic, so the extra-tropical overworld is the source of the entrained air. The entrained air originally entered the overworld through the tropical tropopause, but was transported poleward before being recycled back into the tropical overworld. Thus, it is a reasonable assumption that all air parcels in the overworld entered the stratosphere through the tropical tropopause, and initially had 58±5 ppb CO at θ = 370 K (Figure 3b).

The Northern Hemisphere seasonal distributions of CO in the upper troposphere and lower stratosphere are shown in Figure 4. Each contour plot uses data from at least fifteen ER-2 flights, binned in increments of 20° latitude, 0.5 km altitude, and 10 K potential temperature. For altitudes below 15 km, data are limited to the vicinities of the landing bases at 21°N, 37°N, and 65°N. Figures 4a, 4c, and 4e use pressure altitude as the vertical coordinate. In the stratosphere, isopleths of CO slope downward toward the pole. There is typically 50 to 70 ppb CO at the mid-latitude tropopause, although sometimes less due to stratosphere-troposphere exchange.

To remove the effects of transient motions that result in no net transport, potential temperature is used as the vertical coordinate in Figures 4b, 4d, and 4f. In the stratospheric middleworld (θ < 380 K), there is considerable variability in CO due to stratosphere-troposphere exchange. Isentropes connect the tropical troposphere with the

stratospheric middleworld, allowing adiabatic stratosphere-troposphere exchange [*Holton et al.*, 1995, and references therein]. This exchange causes large variability in middleworld CO [*Lelieveld et al.*, 1997] but does not affect the overworld. CO isopleths are flatter in the overworld than in the middleworld, especially for 400 K < θ < 450 K between 0° and 40°N. The flat isopleths imply that meridional transport is fast relative to photochemical loss of CO between 400 and 450 K. At 60°N, however, there is less CO because of transport out of the Arctic polar vortex. During winter and early spring, strong descent within the vortex brings air parcels with low CO mixing ratios down to the lower stratosphere. In the analysis below, we will compare tropical and mid-latitude data to infer the mean time scale of quasi-horizontal transport out of the tropics.

Analysis

The stratospheric budget of CO is constrained by calculating the rates of reactions (1) and (2) using measured CO, CH_4, OH, temperature, and pressure, and model Cl and $O(^1D)$. Vertical profiles of OH measured by the Harvard HO_x instrument on the ER-2 are shown in Figure 5. It is apparent that in the tropical stratosphere, the OH concentration is not strongly dependent on altitude. However, OH has a strong dependence on solar zenith angle [e.g. *Salawitch et al.*, 1994]. A quadratic fit of tropical OH data to solar zenith angle is used here to calculate a 24-hour mean OH concentration of 7.7×10^5 cm^{-3} in the tropical lower stratosphere. This yields a CO photochemical lifetime of approximately 100 days in the tropics. Uncertainties are approximately ±25% for the OH concentration and ±30% for the rate coefficient of (2) [*W. B. DeMore*, pers. comm.].

Twenty four-hour mean rates of reactions (1) and (2) in the tropics are shown in Figure 6. These rates were calculated from simultaneous measurements of CO and CH_4; 7.7×10^5 cm^{-3} OH; 24-hour mean Cl and $O(^1D)$ from a photochemical model [*Salawitch et al.*, 1994]; and rate coefficients from *DeMore et al.* [1997]. The particular constraints on the photochemical model are described in *Herman et al.* [1998]. Figure 6 illustrates that in the lower stratosphere, the dominant loss of CH_4 is from reaction with OH, but that the relative importance of $O(^1D)$ and Cl increases with altitude. At 50 hPa, the CO mixing ratio is typically 10 to 15 ppb, close to the steady-state balance between reactions (1) and (2). The steady-state mixing ratio increases with temperature due to the temperature-dependence of reaction (1).

The consistency of the OH measurements, rate coefficients, and tropical ascent rates are assessed by modeling tropical CO and comparing with the measured CO. We use a simple model of tropical ascent that only includes diabatic heating and photochemical production and loss of CO:

$$Q\frac{\partial \chi}{\partial \theta} = -L\chi + P \tag{4}$$

where Q is the mass-balanced diabatic heating rate, χ is the CO mixing ratio, L is k_2[OH], P is the rate of (1), and each term is a function of θ (using the annual mean relationship between θ and pressure). Q is the annual mean tropical heating rate calculated from a radiative heating model, with typical uncertainties of 60% for pressures greater than 50 hPa [*Rosenlof*, 1995]. Reaction rates are the same as in Figure 6. In determining tropical CO, photochemical loss dominates entrainment of extra-tropical air, so we do not include entrainment in this model (the results are changed less than 5% by this approximation).

The solution of (4) is superimposed on the tropical CO data in Figure 3b, with a boundary condition of 58 ppb CO at θ = 370 K. There is excellent agreement between predicted and measured CO, validating the OH measurements, rate coefficients, and diabatic heating rates. The dashed lines in Figure 3b represent the error bars corresponding to a 60% uncertainty in the heating rate. The level of agreement between the model and measured CO suggests that the uncertainties are smaller, however it is likely that errors partially cancel. Greater O_3 production would lead to greater diabatic heating and faster ascent (i.e. more CO) but would produce more OH from the $O(^1D)+H_2O$ reaction (i.e. less CO).

The mean time scale for quasi-horizontal transport from the tropics to mid-latitudes can be calculated by comparing CO mixing ratios at the same potential temperature. If we assume that CH_4, pressure, temperature, and the 24-hour mean radical concentrations are constant, then at time t, the CO mixing ratio is given by

$$\chi = P\tau\left(1-\exp\left(-t/\tau\right)\right)+\chi_i \exp\left(-t/\tau\right) \qquad (5)$$

where the CO photochemical lifetime τ is L^{-1}, and χ_i is the initial CO mixing ratio. The product $P\tau$ is the steady-state abundance of CO, which increases with temperature. We will first examine a single flight, and then apply (5) to the annual mean CO profiles.

In the mid-latitude ER-2 flight of 960129 (yymmdd format), there was a constant-altitude flight leg at 14.9 km ($380 < \theta < 385$ K) with H_2O mixing ratios less than 4 parts per million. Air this dry must have entered the stratosphere at the tropical tropopause [*Hintsa et al.*, 1994]. CO and N_2O measured by ALIAS are correlated, as shown in Figure 7. This array of data is a mixing line between tropical and mid-latitude air. The

data with the greatest tropical character has approximately 41 ppb CO and 300 ppb N_2O at $\theta = 381$ K. Extrapolating to the tropical end-member (315 ppb N_2O) yields 52 ppb CO. This mixing ratio is virtually indistinguishable from tropical CO on the same isentropic surface (49.5±2 ppb) due to extremely rapid transport from tropics to mid-latitudes.

We can generalize about transport from the tropics to mid-latitudes by comparing the annual mean CO profiles at different latitudes. Figure 8 shows annual mean stratospheric CO binned by θ and latitude (same bins as in Figure 4). The mid-latitude and tropical profiles are very similar due to rapid quasi-horizontal transport. Solving (5) with the annual mean profiles yields a mean time scale of less than 1 month for isentropic transport from the tropics to mid-latitudes. This time scale does not include the time required for air to ascend from the tropical tropopause to the isentrope of interest, but is in qualitative agreement with independent estimates [e.g. *Boering et al.*, 1995; *Boering et al.*, 1996; *Hintsa et al.*, 1994]. The calculated time scale pertains only to potential temperatures between 380 K and 450 K. At lower potential temperatures, stratosphere-troposphere exchange is significant, and at higher potential temperatures, CO is too similar to steady-state values to infer transport.

Summary

In this paper, we have described the distribution of CO in the upper troposphere and lower stratosphere measured by ALIAS from October 1995 through September 1997. In the upper troposphere, CO has a seasonal cycle with a maximum in the autumn and winter, and a minimum in the spring and summer. During summer in Alaska, however,

upper tropospheric CO is elevated due to an additional source of CO. Over the central tropical Pacific Ocean, upper tropospheric CO is 60±5 ppb with little seasonal variation. In the tropical lower stratosphere, CO decreases as potential temperature increases, with small seasonal variations. A simple model can reproduce the measured tropical profile of CO with 7.7×10^5 cm^{-3} OH (24-hour mean) inferred from measured OH and diabatic heating rates from a radiative heating model.

Contour plots of CO have flat isopleths at potential temperatures between 400 and 450 K due to rapid transport from the tropical to mid-latitude stratosphere. The mean time scale of this transport is calculated to be less than one month. Thus, in this region of the stratosphere, a large volume of tropical air is being transported to the mid-latitude overworld. Since this air has only recently entered the stratosphere, it has relatively large concentrations of CO and potentially other reactive species that could affect mid-latitude stratospheric O_3 abundances.

Acknowledgments

We thank J. P. Pinto and S. C. Wofsy for helpful discussions; B. L. Gary for the use of unpublished data; E. J. Hintsa for H_2O data; K. H. Rosenlof for providing tropical heating rates; G. J. Flesch, L. Kroll, K. Modarress, and M. Tuchscherer for laboratory and field support of the ALIAS instrument; the ER-2 pilots and crew; and A. E. Kulawik for computational assistance. This work was supported by NASA's Upper Atmospheric Research Program (UARP) and the Atmospheric Effects of Aviation Project (AEAP). Part of the research described in this paper was carried out by the Jet Propulsion

Laboratory, California Institute of Technology, under a contract with the National Aeronautics and Space Administration.

References

Anderson, B. E., J. E. Collins, G. W. Sachse, G. W. Whiting, D. R. Blake, and F. S. Rowland, AASE-II Observations of Trace Carbon Species Distributions in the Mid to Upper Troposphere, *Geophys. Res. Let.*, 20, 2539-42, 1993.

Boering, K. A., E. J. Hintsa, S. C. Wofsy, J. G. Anderson, B. C. Daube, Jr., A. E. Dessler, M. Loewenstein, M. P. McCormick, J. R. Podolske, E. M. Weinstock, and G. K. Yue, Measurements of stratospheric carbon dioxide and water vapor at northern midlatitudes: Implications for troposphere-to-stratosphere transport, *Geophys. Res. Let.*, 22, 2737-40, 1995.

Boering, K. A., S. C. Wofsy, B. C. Daube, H. R. Schneider, M. Loewenstein, J. R. Podolske, and T. J. Conway, Stratospheric Mean Ages and Transport Rates from Observations of Carbon Dioxide and Nitrous Oxide, *Science*, 274, 1340-3, 1996.

Bregman, A., F. Arnold, V. Bürger, H. Fischer, J. Lelieveld, B. A. Scheeren, J. Schneider, P. C. Siegmund, J. Ström, A. Waibel, and W. M. F. Wauben, In Situ Trace Gas and Particle Measurements in the Summer Lower Stratosphere during STREAM II: Implications for O_3 Production, *J. Atmos. Chem.*, 26, 275-310, 1997.

Crutzen, P. J., Ozone in the troposphere, in *Composition, Chemistry, and Climate of the Atmosphere*, H. B. Singh, ed., 349-93, Van Nostrand Reinhold, New York, 1995.

DeMore, W. B., S. P. Sander, D. M. Golden, R. F. Hampson, M. J. Kurylo, C. J. Howard, A. R. Ravishankara, C. E. Kolb, and M. J. Molina, Chemical Kinetics and Photochemical Data for Use in Stratospheric Modeling, JPL Publication 97-4, 1997.

Denning, R. F., S. L. Guidero, G. S. Parks, and B. L. Gary, Instrument description of the airborne Microwave Temperature Profiler, *J. Geophys. Res.*, 94, 16757-65, 1989.

Harriss, R. C., G. W. Sachse, and G. F. Hill, Carbon Monoxide and Methane in the North American Arctic and Sub-Arctic, *J. Geophys. Res.*, 97, 16589-99, 1992.

Herman, R. L., D. C. Scott, C. R. Webster, R. D. May, E. J. Moyer, R. J. Salawitch, Y. L. Yung, G. C. Toon, B. Sen, J. J. Margitan, K. H. Rosenlof, H. A. Michelsen, J. W. Elkins, Tropical Entrainment Time Scales Inferred from Stratospheric N_2O and CH_4 Observations, submitted to *Geophys. Res. Let.*, 1998.

Hintsa, E. J., E. M. Weinstock, A. E. Dessler, J. G. Anderson, M. Loewenstein, and J. R. Podolske, SPADE H_2O measurements and the seasonal cycle of stratospheric water vapor, *Geophys. Res. Let.*, 21, 2559-62, 1994.

Hipskind, R. S., G. L. Gregory, G. W. Sachse, G. F. Hill, and E. F. Danielson, Correlations Between Ozone and Carbon Monoxide in the Lower Stratosphere, Folded Tropopause, and Maritime Troposphere, *J. Geophys. Res.*, 92, 2121-30, 1987.

Holton, J. R., P. H. Haynes, M. E. McIntyre, A. R. Douglass, R. B. Rood, and L. Pfister, Stratosphere-Troposphere Exchange, *Rev. Geophys.*, 33, 403-39, 1995.

Hoor, P., R. Konigstedt, U. Parchtka, F. G. Wienhold, and H. Fischer, Measurements of CO in the Arctic Lower Stratosphere During Winter 1996/7, *Chemosphere*, this issue, 1998.

Hoskins, B. J., Towards a PV-theta view of the general circulation, *Tellus, Ser. A.*, 43, 27-35, 1991.

Lelieveld, J., B. Bregman, F. Arnold, V. Bürger, P. J. Crutzen, H. Fischer, A. Waibel, P. Siegmund, P. F. J. van Velthoven, Chemical perturbation of the lowermost stratosphere through exchange with the troposphere, *Geophys. Res. Let.*, 24, 603-6, 1997.

Levy, H., II, Normal atmosphere: Large radical and formaldehyde concentrations predicted, *Science*, 173, 141-3, 1971.

Logan, J. A., M. J. Prather, S. C. Wofsy, and M. B. McElroy, Tropospheric Chemistry: A Global Perspective, *J. Geophys. Res.*, 86, 7210-54, 1981.

May, R. D., Open-Path Near-Infrared Tunable Diode Laser Spectrometer for Atmospheric Measurements of H_2O, submitted to *J. Geophys. Res.*, 1998.

May, R. D. and C. R. Webster, Data processing and calibration for tunable diode laser harmonic absorption spectrometers, *J. Quant. Spectrosc. Radiat. Transfer*, 49, 335-347, 1993.

Pinto, J. P., Y. L. Yung, D. Rind, G. L. Russell, J. A. Lerner, J. E. Hansen, and S. Hameed, A General Circulation Model Study of Atmospheric Carbon Monoxide, *J. Geophys. Res.*, 88, 3691-702, 1983.

Pressman, J., and P. Warneck, The stratosphere as a chemical sink for carbon monoxide, *J. Atm. Sci.*, 27, 155-63, 1970.

Proffitt, M. H., and R. J. McLaughlin, Fast-response dual-beam UV-absorption ozone photometer suitable for use on stratospheric balloons, *Rev. Sci. Instrum.*, 54, 1719-28, 1983.

Reid, G. C., and K. S. Gage, The tropical tropopause over the western Pacific: wave driving, convection, and the annual cycle, *J. Geophys. Res.*, 101, 21233-41, 1996.

Robinson, E., D. Clark, and W. Seiler, The Latitudinal Distribution of Carbon Monoxide Across the Pacific from California to Antarctica, *J. Atmos. Chem.*, 1, 137-49, 1984.

Rosenlof, K. H., Seasonal cycle of the residual mean meridional circulation in the stratosphere, *J. Geophys. Res.*, 100, 5173-91, 1995.

Salawitch, R. J., et al., The diurnal variation of hydrogen, nitrogen, and chlorine radicals: implications for the heterogeneous production of HNO_2, *Geophys. Res. Lett.*, 21, 2551-4, 1994.

Scott, S. G., T. P. Bui, K. R. Chan, and S. W. Bowen, The Meteorological Measurement System on the NASA ER-2 aircraft, *J. Atmos. and Oceanic Technol.*, 7, 525-40, 1990.

Tuck, A. F., et al., The Brewer-Dobson circulation in the light of high altitude *in situ* aircraft observations, *Quart. J. Roy. Met. Soc.*, 123, 1-69, 1997.

Volk, C. M., J. W. Elkins, D. W. Fahey, R. J. Salawitch, G. S. Dutton, J. M. Gilligan, M. H. Proffit, M. Loewenstein, J. R. Podolske, K. Minschwaner, J. J. Margitan, and K. R. Chan, Quantifying transport between the tropical and mid-latitude lower stratosphere, *Science*, 272, 1763-8, 1996.

Waibel, A. E., H. Fischer, P. C. Siegmund, B. Lee, F. G. Wienhold, P. J. Crutzen, J. Lelieveld, and J. Strom, Highly elevated carbon monoxide concentrations in the upper troposphere and lowermost stratosphere at northern midlatitudes during STREAM II summer campaign in 1994, *Chemosphere*, this issue, 1998.

Webster, C. R., R. D. May, C. A. Trimble, R. G. Chave, and K. Kendall, Aircraft (ER-2) laser infrared absorption spectrometer (ALIAS) for *in situ* stratospheric measurements of HCl, N_2O, CH_4, NO_2 and HNO_3, *Appl. Opt.*, 33, 454-472, 1994.

Weinstock, E. M., E. J. Hintsa, J. G. Anderson, K. A. Boering, B. C. Daube, S. C. Wofsy, R. L. Herman, R. D. May, C. R. Webster, and T. P. Bui, Evaluation of the seasonal cycle of water vapor in the stratosphere from monthly average tropical tropopause temperatures using a CO photochemical clock, in preparation, 1998.

Weinstock, E. M., E. J. Hintsa, A. E. Dessler, J. F. Oliver, N. L. Hazen, J. N. Demusz, N. T. Allen, L. B. Lapson, and J. G. Anderson, A new fast response photofragment fluorescence hygrometer for use on the NASA ER-2 and Perseus remotely piloted aircraft, *Rev. Sci. Instrum.*, 65, 3544-54, 1994.

Wennberg, P. O., R. C. Cohen, N. L. Hazen, L. B. Lapson, N. T. Allen, T. F. Hanisco, J. F. Oliver, N. W. Lanham, J. N. Demusz, and J. G. Anderson, Aircraft-borne, laser-induced fluorescence instrument for the *in situ* detection of hydroxyl and hydroperoxyl radicals, *Rev. Sci. Instrum.*, 65, 1858-76, 1994.

Wennberg, P. O., et al., Hydrogen Radicals, Nitrogen Radicals, and the Production of O_3 in the Upper Troposphere, *Science*, 279, 49-53, 1998.

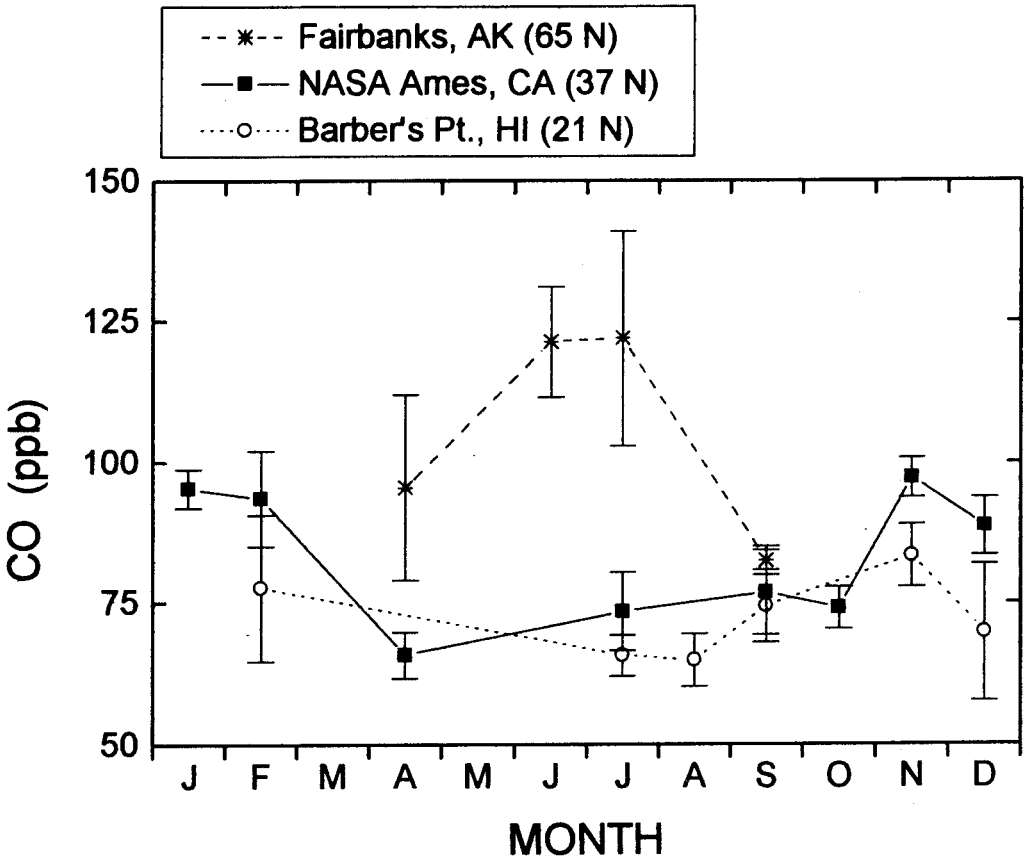

Figure 1. Upper tropospheric CO measured by ALIAS between 7 km altitude and the local tropopause minus 1 km. Symbols are monthly means (±1 st. dev.). Instrument precision is ±0.7 ppb, so the observed scatter within each monthly bin is caused by atmospheric variation.

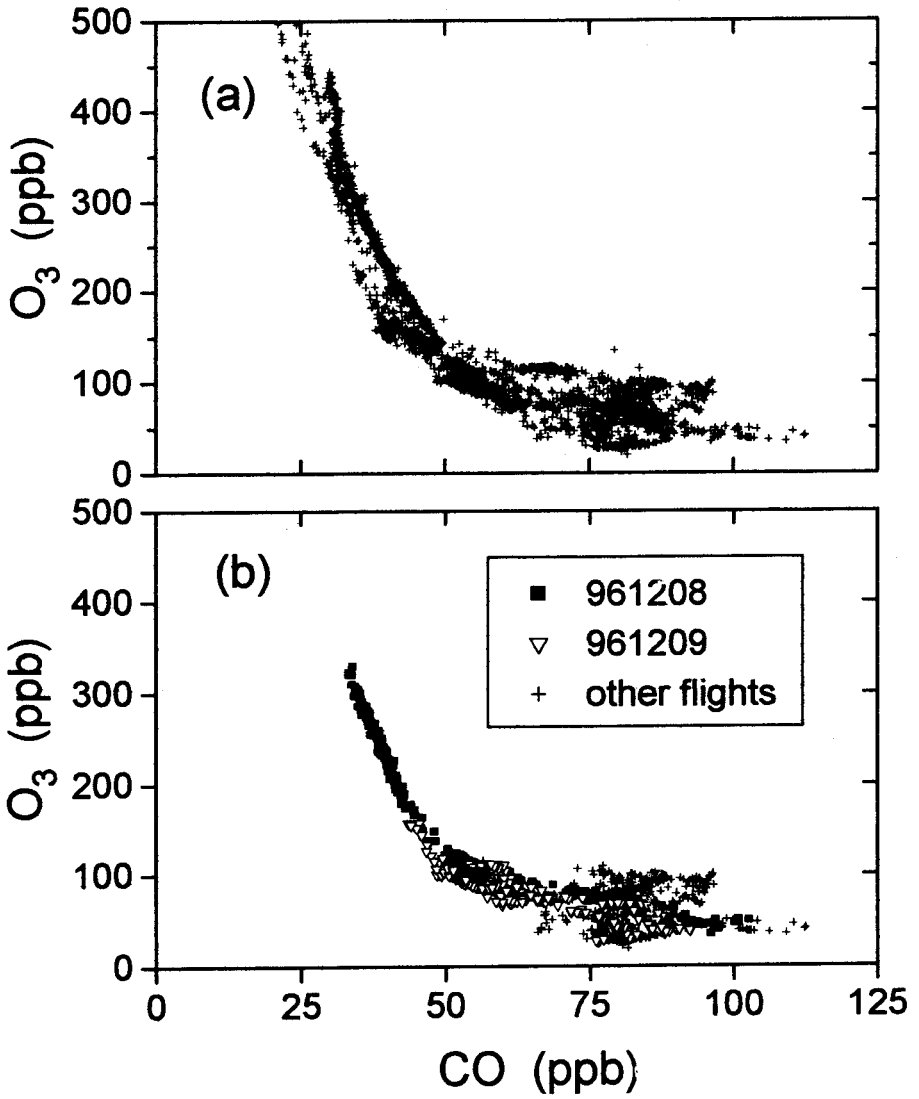

Figure 2. O_3 *vs.* CO measured over Hawaii (21°N) in November, 1995, and December, 1996. (a) All data: O_3 and CO are anticorrelated in the lower stratosphere. (b) Tropospheric data more than 1 km below the local tropopause: no correlation is apparent except for the flights of 961208 and 961209 (yymmdd format). On these two days, there is evidence that stratospheric air has recently intruded into the upper troposphere.

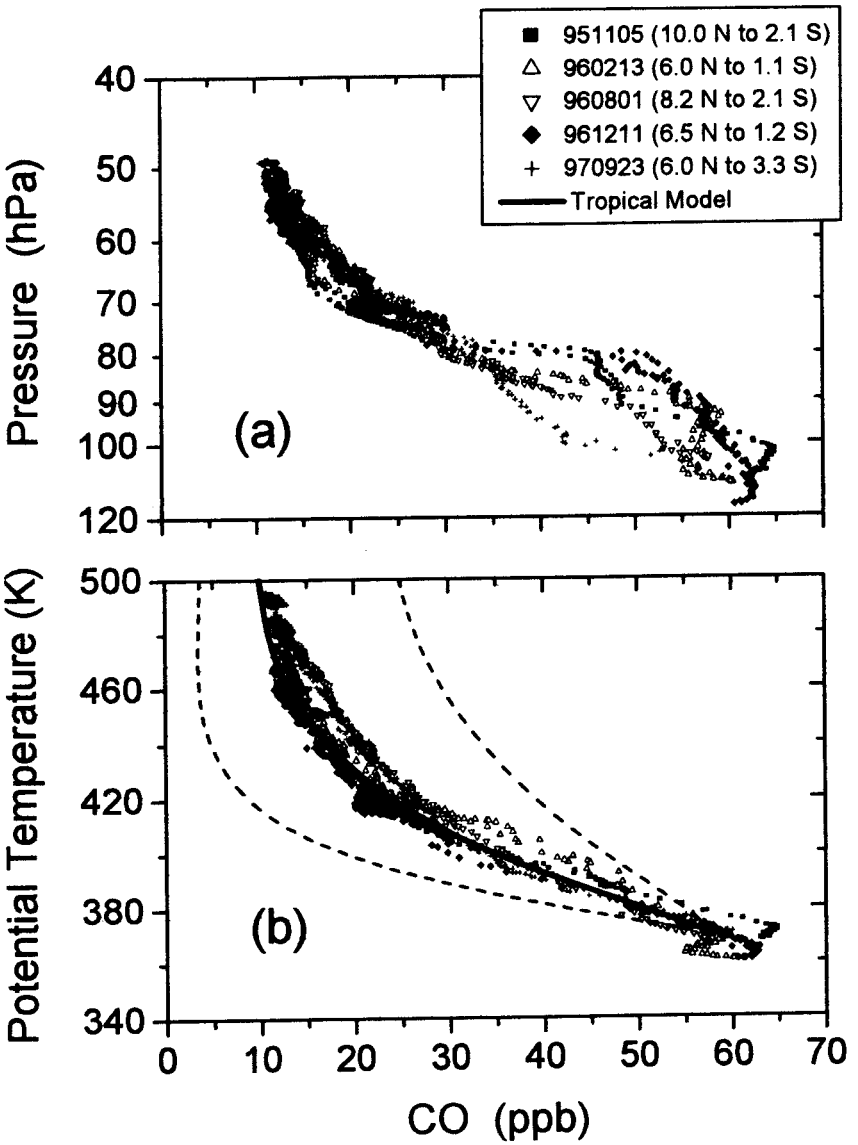

Figure 3. Tropical CO profiles measured by ALIAS. (a) CO fluctuates as a function of pressure, depending on the height of the tropopause. (b) As a function of potential temperature, θ, CO has the same vertical profile throughout the year, with a tropical tropopause at 370±10 K (approximately 15.5 to 17.2 km). Solid line is tropical model CO and dashed lines represent typical uncertainty in ascent rate.

Figure 4. (on following pages) ALIAS CO distribution (ppb) in the upper troposphere and lower stratosphere of the Northern Hemisphere. These plots represent seasonal averages created by binning the data every 20° latitude and 0.5 km altitude (or 10 K potential temperature): (a) Winter 1996 and Spring 1997 altitude vs. latitude (15 flights), (b) Winter 1996 and Spring 1997 potential temperature vs. latitude (15 flights), (c) Summer 1996 and 1997 altitude vs. latitude (21 flights), (d) Summer 1996 and 1997 potential temperature vs. latitude (21 flights), (e) Autumn 1995, 1996, and 1997 altitude vs. latitude (21 flights), (f) Autumn 1995, 1996, and 1997 altitude vs. latitude (21 flights).

Fig. 4a: Winter 1996 and Spring 1997

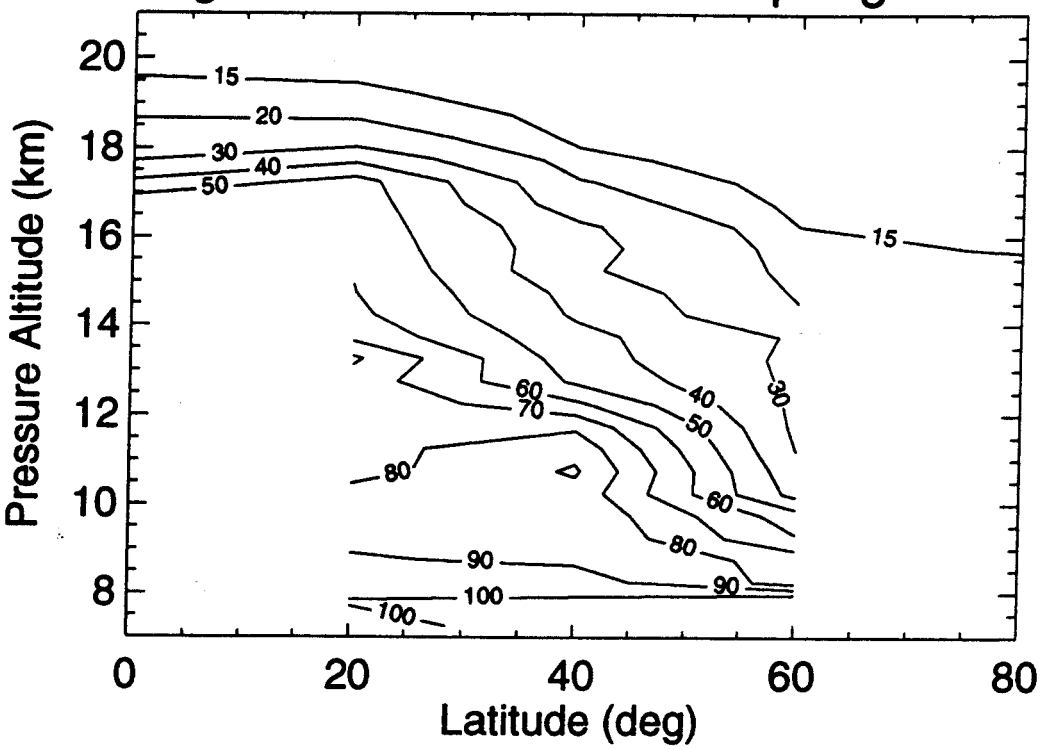

Fig. 4b: Winter 1996 and Spring 1997

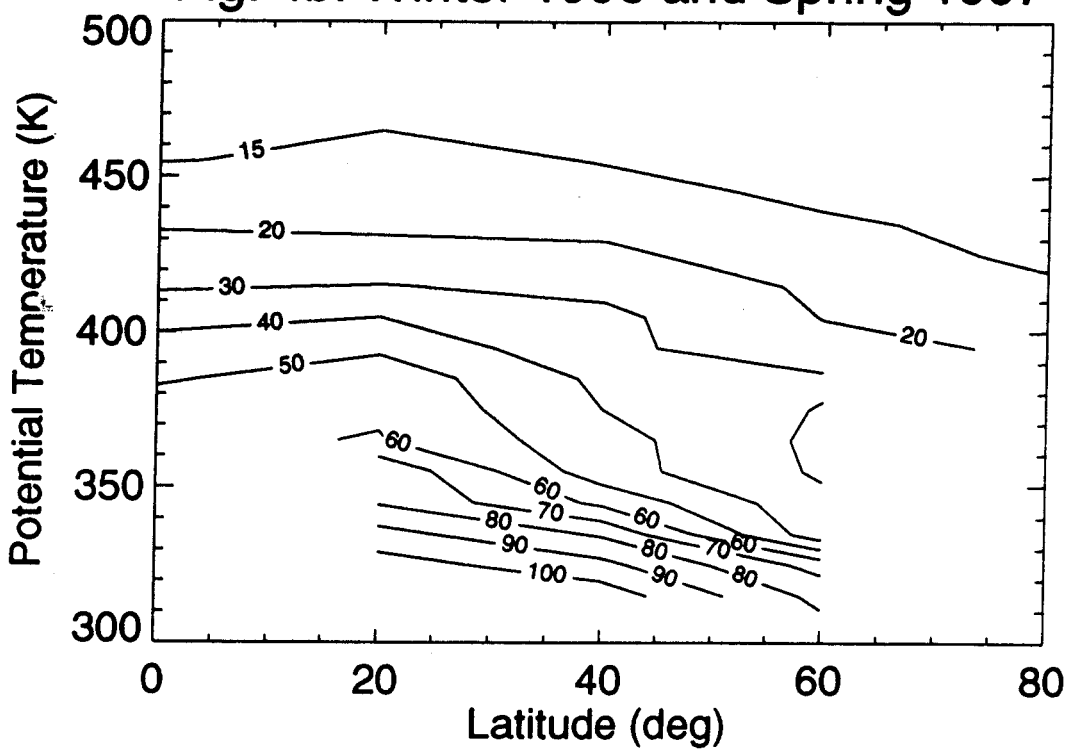

Fig. 4c: Summer 1996 and 1997

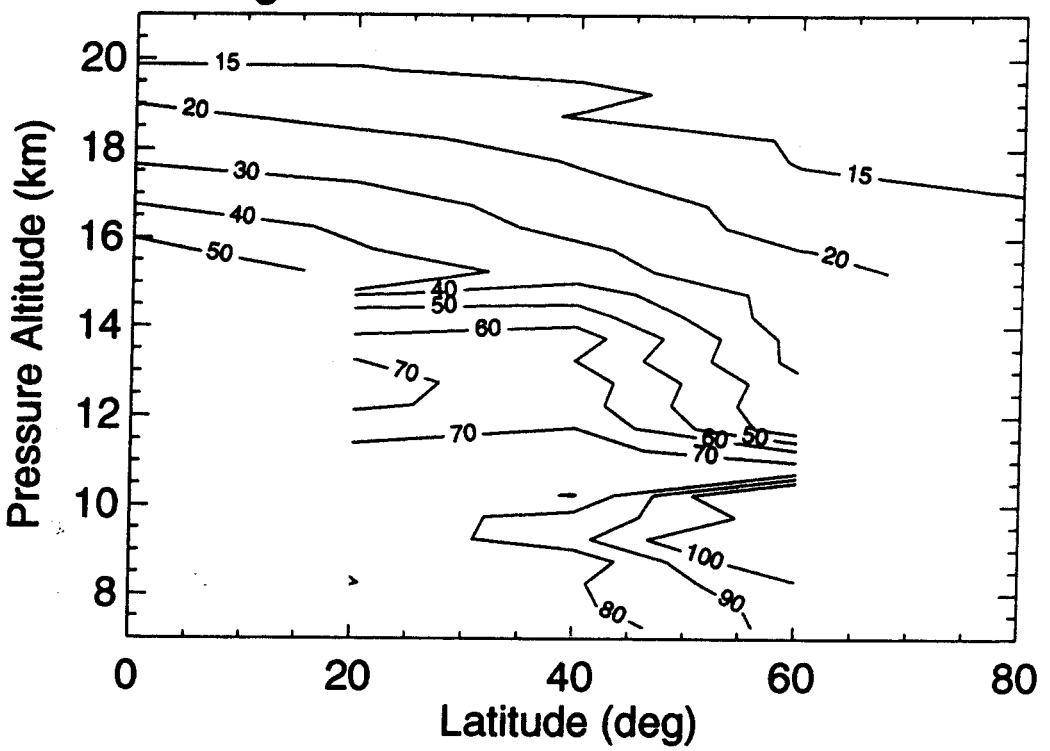

Fig. 4d: Summer 1996 and 1997

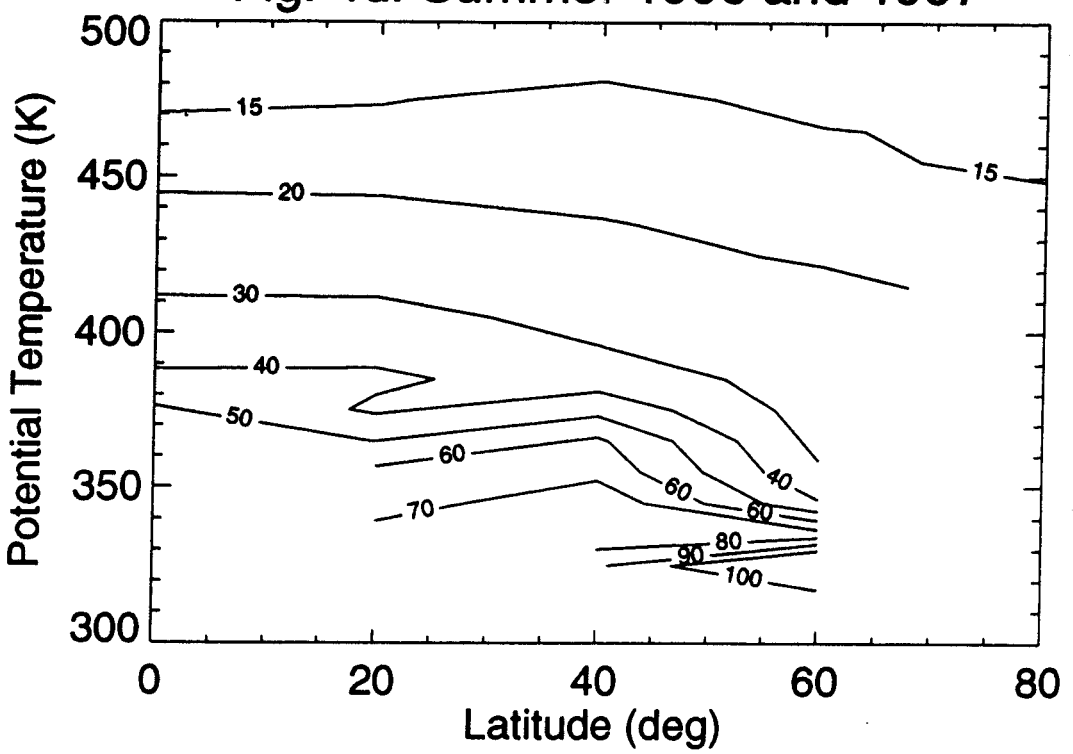

Fig. 4e: Autumn 1995, 1996, 1997

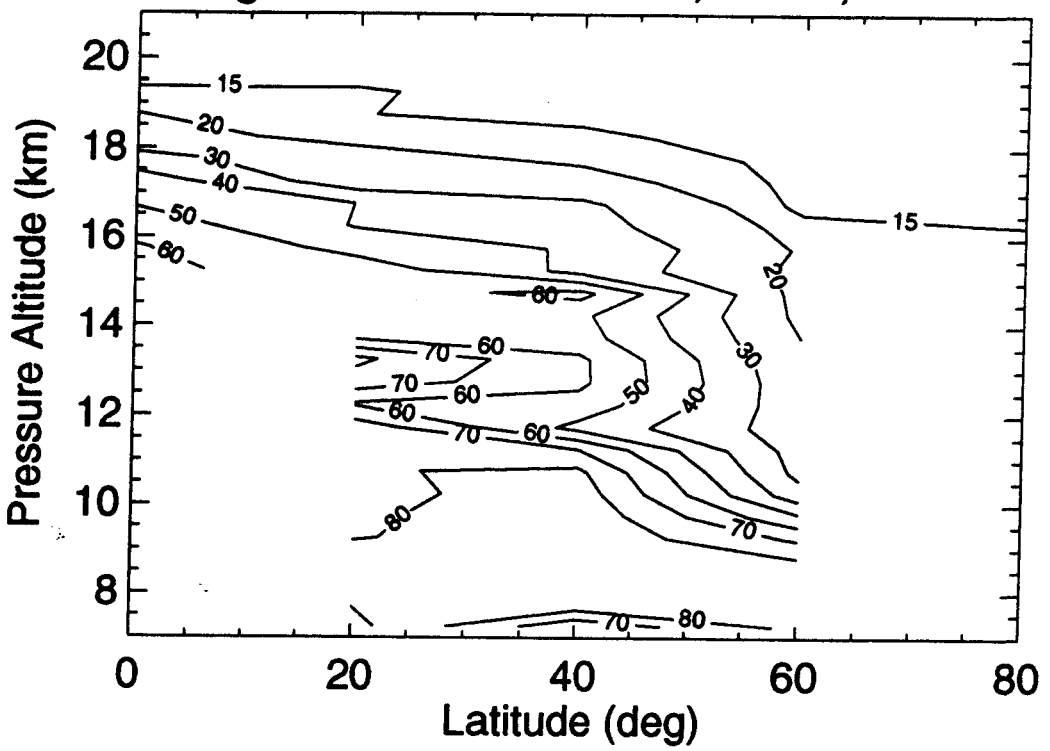

Fig. 4f: Autumn 1995, 1996, 1997

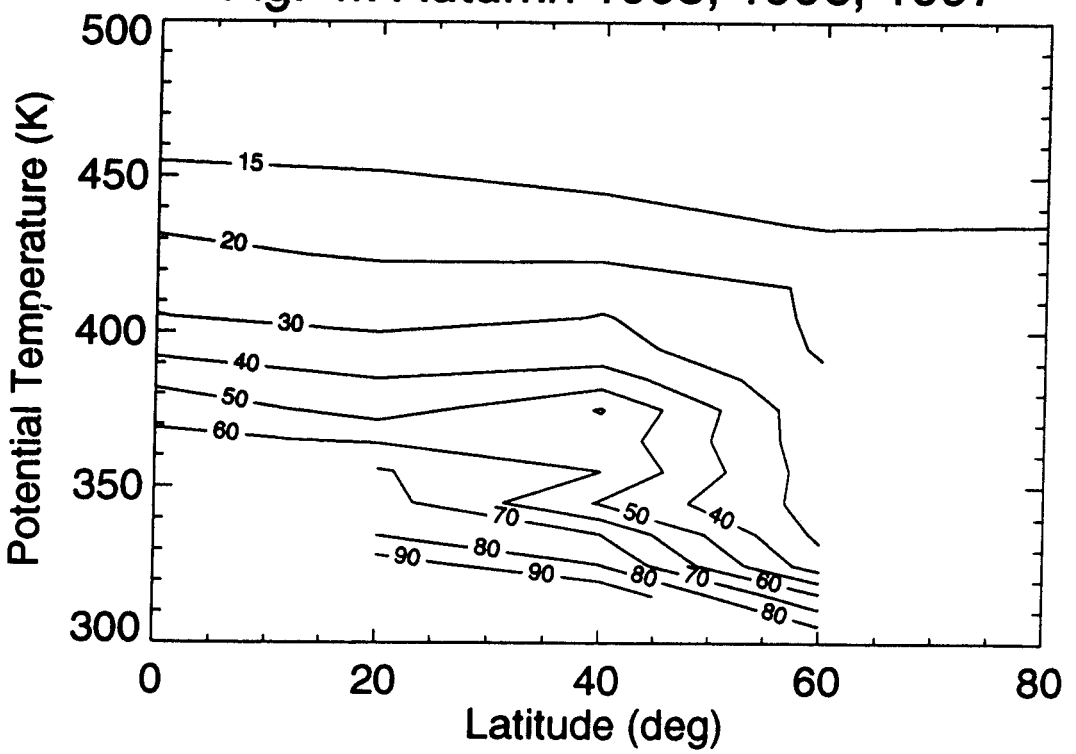

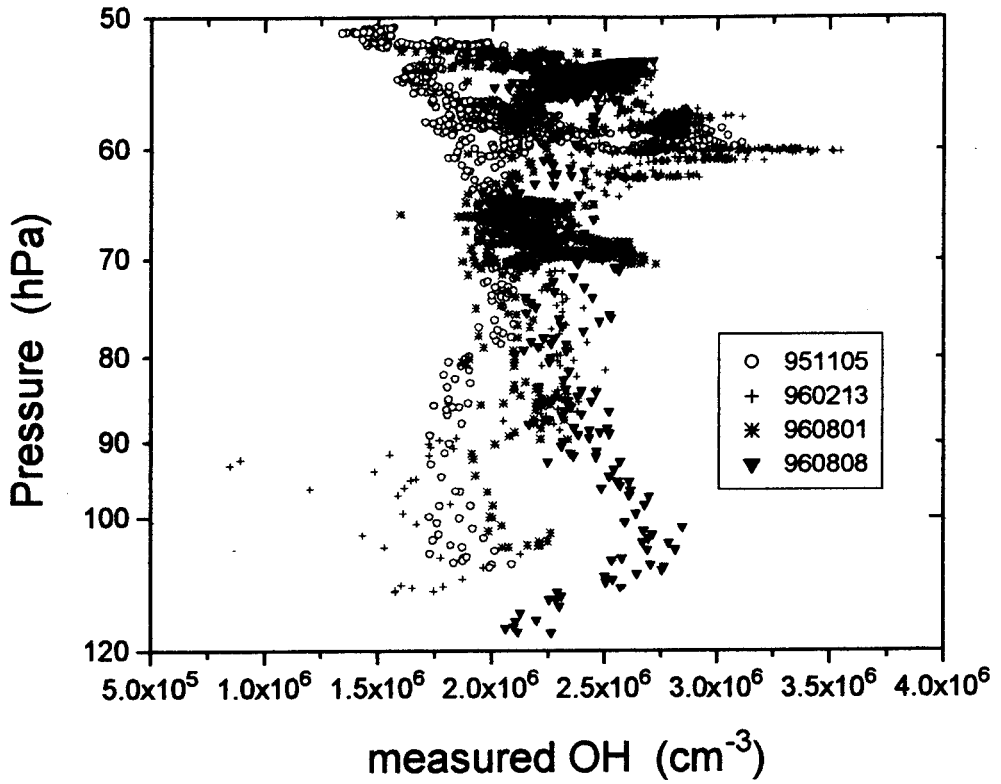

Figure 5. OH measurements from Harvard HO_x taken during tropical ER-2 flights. Latitudes are the same as in Figure 3.

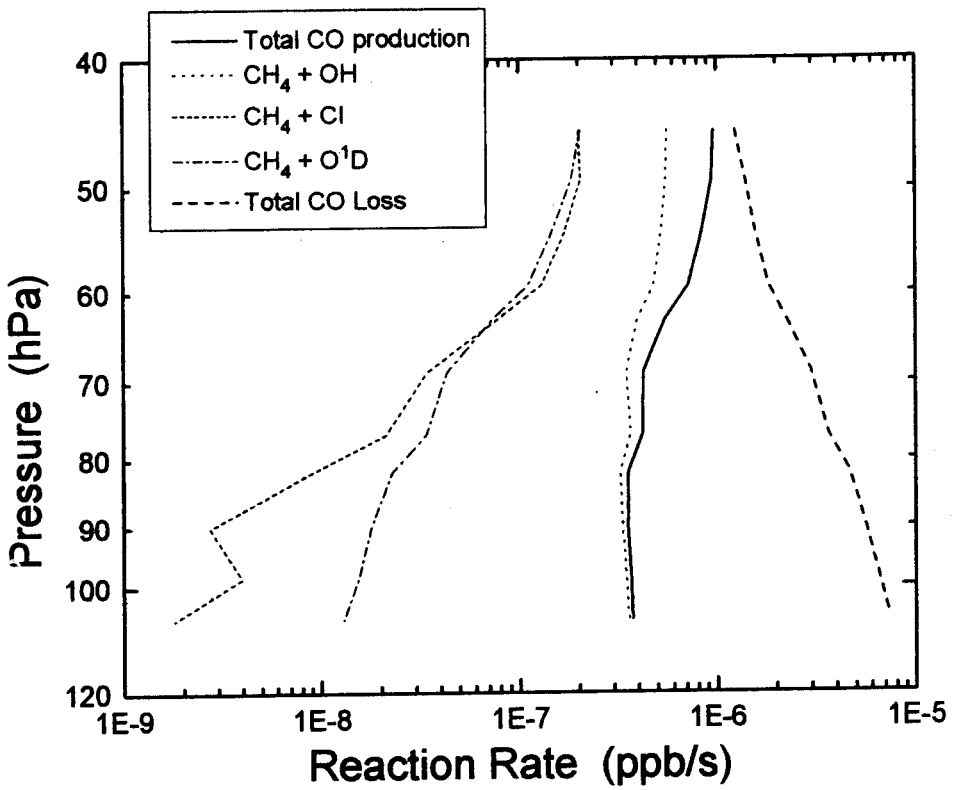

Figure 6. CO production and loss rates in the tropics. The rates were calculated from mean measured profiles of CO and CH_4, 24-hour mean Cl and $O(^1D)$ from a photochemical model [*Salawitch et al.*, 1994], and 24-hour mean OH (7.7×10^5 cm^{-3}) inferred from an empirical relationship between measured OH and solar zenith angle.

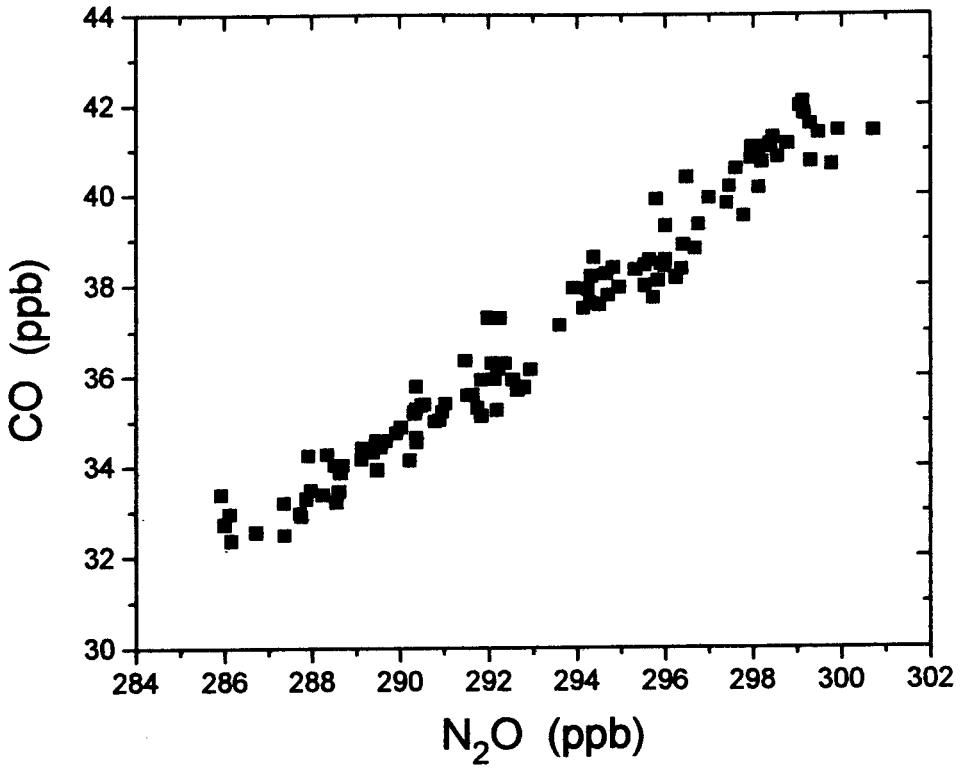

Figure 7. Measured CO *vs.* N_2O from a constant-altitude flight leg (14.9 km, 122-3 hPa, $380 < \theta < 385$ K) during the 960129 ER-2 mid-latitude flight. This is a mixing line with a tropical end-member of 52 ppb CO and 315 ppb N_2O.

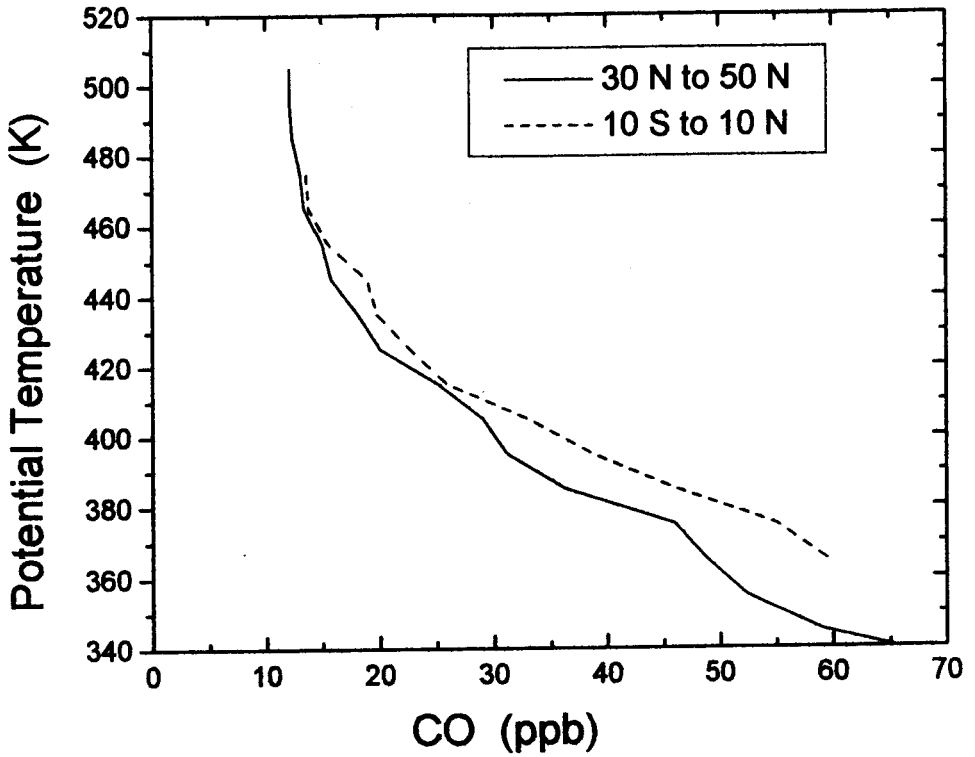

Figure 3. Annual mean stratospheric CO profiles, binned by potential temperature.